

Measurement of apparent ion temperature using the magnetic recoil spectrometer at the OMEGA laser facility

M. Gatu Johnson, J. Katz, C. Forrest, J. A. Frenje, V. Yu. Glebov, C. K. Li, R. Paguio, C. E. Parker, C. Robillard, T. C. Sangster, M. Schoff, F. H. Séguin, C. Stoeckl, and R. D. Petrasso

Citation: [Review of Scientific Instruments](#) **89**, 101129 (2018); doi: 10.1063/1.5035287

View online: <https://doi.org/10.1063/1.5035287>

View Table of Contents: <http://aip.scitation.org/toc/rsi/89/10>

Published by the [American Institute of Physics](#)



PFEIFFER VACUUM

VACUUM SOLUTIONS FROM A SINGLE SOURCE

Pfeiffer Vacuum stands for innovative and custom vacuum solutions worldwide, technological perfection, competent advice and reliable service.

[Learn more!](#)

The advertisement features a black background with several pieces of vacuum equipment. On the left, there is a red and silver cylindrical device with a control panel. In the center, a smaller red and silver component is shown. On the right, a larger, more complex silver and red machine is visible. The Pfeiffer Vacuum logo is at the top left, and the main headline is in large white letters on a red background. Below the headline is a short paragraph of text and a 'Learn more!' button.

Measurement of apparent ion temperature using the magnetic recoil spectrometer at the OMEGA laser facility

M. Gatu Johnson,^{1,a)} J. Katz,² C. Forrest,² J. A. Frenje,¹ V. Yu. Glebov,² C. K. Li,¹ R. Paguio,³ C. E. Parker,¹ C. Robillard,² T. C. Sangster,² M. Schoff,³ F. H. Séguin,¹ C. Stoeckl,² and R. D. Petrasso¹

¹*Massachusetts Institute of Technology Plasma Science and Fusion Center, Cambridge, Massachusetts 02139, USA*

²*Laboratory for Laser Energetics, University of Rochester, Rochester, New York 14623, USA*

³*General Atomics, San Diego, California 92186, USA*

(Presented 16 April 2018; received 13 April 2018; accepted 5 June 2018; published online 11 October 2018)

The Magnetic Recoil neutron Spectrometer (MRS) at the OMEGA laser facility has been routinely used to measure deuterium-tritium (DT) yield and areal density in cryogenically layered implosions since 2008. Recently, operation of the OMEGA MRS in higher-resolution mode with a new smaller, thinner (4 cm², 57 μm thick) CD₂ conversion foil has also enabled inference of the apparent DT ion temperature (T_{ion}) from MRS data. MRS-inferred T_{ion} compares well with T_{ion} as measured using neutron time-of-flight spectrometers, which is important as it demonstrates good understanding of the very different systematics associated with the two independent measurements. The MRS resolution in this configuration, $\Delta E_{\text{MRS}} = 0.91$ MeV FWHM, is still higher than that required for a high-precision T_{ion} measurement. We show how fielding a smaller foil closer to the target chamber center and redesigning the MRS detector array could bring the resolution to $\Delta E_{\text{MRS}} = 0.45$ MeV, reducing the systematic T_{ion} uncertainty by more than a factor of 4. *Published by AIP Publishing.*
<https://doi.org/10.1063/1.5035287>

I. INTRODUCTION

Neutron spectrometers provide the essential performance parameters of yield, areal density (ρR), and apparent plasma ion temperature (T_{ion}) from inertial confinement fusion (ICF) implosions. On the OMEGA laser facility,¹ two types of neutron spectrometers are employed: a Magnetic Recoil neutron Spectrometer (MRS)^{2–6} and neutron Time-of-Flight (nTOF) spectrometers.^{7–9} The OMEGA MRS has been routinely used to measure deuterium-tritium (DT) yield and areal density in cryogenically layered implosions since 2008, but has up until now not been used for T_{ion} measurements due to low spectrometer energy resolution.⁶ The MRS design requires a trade-off between efficiency and resolution, and efficiency was prioritized because of relatively low anticipated implosion yields. However, recently yields for cryogenically layered DT implosions on OMEGA have climbed above 10¹⁴ (Ref. 10), concurrently with a growing interest in precision T_{ion} measurements as a key to understanding implosion performance. Thermal T_{ion} is an essential parameter for determining achieved hot-spot pressure, which is the primary metric used to gauge progress toward ignition.¹¹ This is complicated by the fact that apparent T_{ion} as inferred from the broadening of measured burn-averaged neutron spectra¹² will be inflated relative to thermal by any residual fuel motion at burn.^{13–15} Low-mode asymmetries have materialized as one of the primary

challenges to ICF ignition.^{16–18} These low-mode asymmetries induce flows in the burning fuel and can manifest as T_{ion} asymmetries. nTOF measurements of the primary DT neutron spectrum at OMEGA show evidence of such asymmetries,¹⁹ which are important to control and understand.

Together, the recent increase in yields at OMEGA and the renewed interest in precision T_{ion} measurements motivated the present study, which is aimed at (i) evaluating achievable T_{ion} measurement quality with the current MRS and (ii) identifying steps toward further improving this measurement. Note that a similar MRS installed on the National Ignition Facility²⁰ has been reporting T_{ion} since 2011,²¹ recently with significantly improved precision.²² T_{ion} on OMEGA is currently only measured using nTOF detectors, and complementary high-precision measurements using a different technique would be very valuable. The paper is organized as follows. In Sec. II, the MRS concept and factors impacting instrument response are briefly introduced. In Sec. III, measurements of apparent T_{ion} using the current MRS in high-resolution mode are presented and uncertainties reviewed. Section IV discusses paths toward further improving instrument resolution and reducing uncertainty in MRS T_{ion} measurements. Section V concludes the paper.

II. MRS INSTRUMENT RESPONSE

The OMEGA MRS setup, described in detail in Ref. 6, is illustrated in Fig. 1. Briefly, a fraction of the neutrons emitted at the target chamber center (TCC) scatter elastically in the CD₂ conversion foil, generating recoil deuterons. A fraction of the

Note: Paper published as part of the Proceedings of the 22nd Topical Conference on High-Temperature Plasma Diagnostics, San Diego, California, April 2018.

^{a)} Author to whom correspondence should be addressed: gatu@psfc.mit.edu.

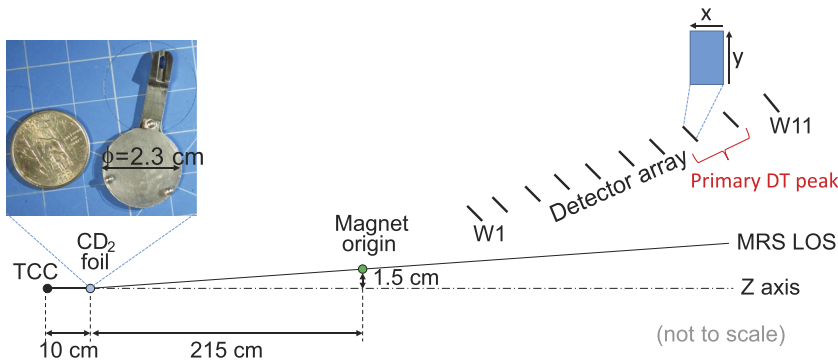


FIG. 1. Cartoon of the MRS setup (not to scale), illustrating the primary system components: a CD_2 conversion foil, a bending magnet, and a CR-39 detector array. The picture inset shows the new 4 cm^2 , $57.2 \mu\text{m}$ thick foil used in the measurements for this paper. The cartoon inset illustrates the geometry of and coordinate system for each individual CR-39 detector.

recoil deuterons are selected by an aperture behind the target chamber wall and are momentum separated by a permanent bending magnet to be detected in a different physical location on the CR-39 detector array depending on their energy. The measured signal distribution is used to reconstruct a recoil deuteron energy spectrum, from which the neutron spectrum is subsequently inferred.

The MRS response is simulated using the Geant4²³ toolkit. In principle, the response can be fully calculated *ab initio* based on the known system geometry. However, as discussed in Ref. 6, the simulated response has to be verified *in situ* to ensure it captures the as-built geometry. This is particularly important for a precision measurement of T_{ion} . In Fig. 2, measured MRS primary 14 MeV DT-neutron peak signal distributions in the dispersion direction (x) and the non-dispersion direction (y) are contrasted to Geant4 simulations. The dashed lines represent simulations using the old best understanding of the as-built MRS geometry as described in Ref. 6. These simulations assumed that the foil insertion mechanism partially blocked the recoil deuteron path from the foil to the aperture. This assumption could not be verified in the detailed CAD modeling of the setup and was hence abandoned. However, from Fig. 2(b), it is clear that the observed signal distribution is asymmetric in the non-dispersion (y) direction. The new hypothesis for this is a systematic setup misalignment in the non-dispersion direction. Simulations show that the signal distribution in the non-dispersion direction is well captured by a 0.6 cm foil misalignment in this direction [solid line in Fig. 2(b)].

When comparing the old best Geant4 simulations (dashed line) with the measured signal distributions in the dispersion direction [Fig. 2(a)], it is clear that the simulations do not capture the behavior of the signal in the “shadow region,” where W10 is shadowed by W9 (see Fig. 1). It turns out that the reason for this is that while MRS was intended to be built with the detectors located in a specified location relative to the Z axis in Fig. 1, the as-built geometry has the detectors in the same location relative instead to the MRS line-of-sight (LOS) as defined in Fig. 1. When the as-built detector geometry relative to the magnet is implemented in the Geant4 simulations, the shadow region is well captured [solid line in Fig. 2(a)]. However, this unintended implementation of the detectors means that they are not ideally located in the focal plane of the magnet.

The optimized Geant4 simulations of the MRS setup used in this paper implement a systematic 0.6 cm foil misalignment in the non-dispersion direction and the as-built detector

locations. These simulations describe measured data very well (solid lines in Fig. 2).

The MRS efficiency is determined by the solid angle covered by the foil and aperture, the number of deuterons in the foil (thickness and density), and the n, D elastic scattering cross section.⁶ The MRS resolution can be separated into three main components: kinematic broadening (ΔE_{kin}), due to the kinematics of n, D elastic scattering, foil broadening (ΔE_{foil}), due to recoil deuteron energy loss in the foil, and magnet broadening (ΔE_{mag}), due to the ion optical properties of the magnet;

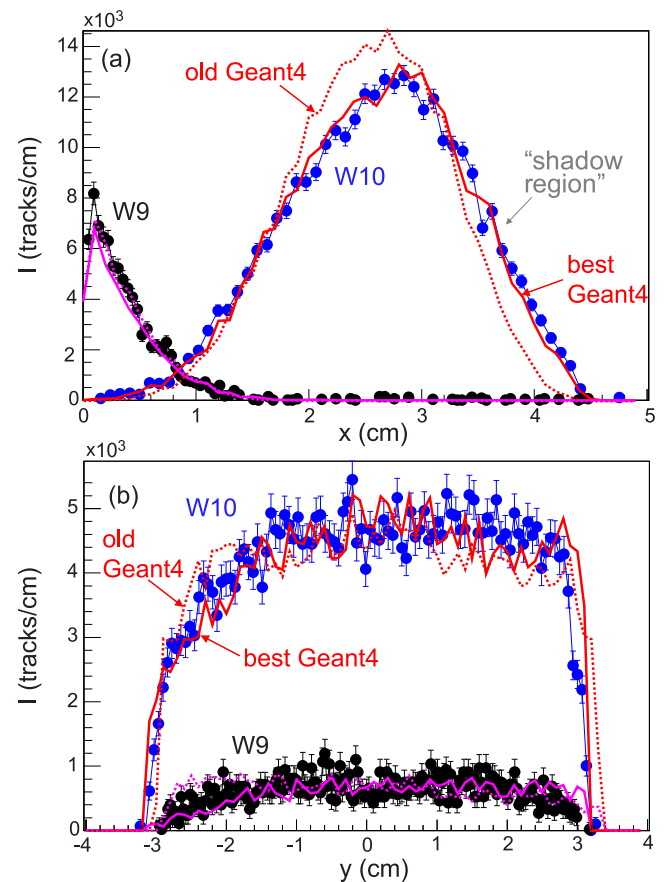


FIG. 2. Measured (points with error bars) and Geant4-simulated (lines) primary 14 MeV DT peak signal distributions in (a) the dispersion direction and (b) the non-dispersion direction on individual W9 and W10 CR-39 coupons when the 4 cm^2 , $57.2 \mu\text{m}$ thick CD_2 foil is used. The dotted curves represent simulations assuming the old best understanding of the as-built MRS geometry (Ref. 6), while the solid curves represent the current best understanding used in the analysis for this paper.

$\Delta E_{\text{MRS}} = \sqrt{(\Delta E_{\text{kin}}^2 + \Delta E_{\text{foil}}^2 + \Delta E_{\text{mag}}^2)}$. The kinematic broadening is determined by the spread in scattering angles and is dominated by the foil opening angle. The foil broadening is directly determined by foil thickness.

III. TION MEASUREMENTS WITH THE EXISTING SYSTEM

To test the capability of measuring T_{ion} , the MRS resolution was optimized by fielding a new 4 cm², 57.2 μm thick CD₂ foil (Fig. 1). In this configuration, the efficiency is 2.1×10^{-10} and the FWHM resolution $\Delta E_{\text{MRS}} = 0.91$ MeV. MRS was fielded with the new foil on a series of implosions with T_{ion} as measured by the nTOF detectors ranging from 4.3 to 12.0 keV and DT yields ranging from 1.3×10^{13} to 1.4×10^{14} . These were all warm target implosions specifically designed for calibration purposes, with negligible ρR and no remaining kinetic energy at burn, hence with no expected T_{ion} asymmetries. The assumption of no remaining kinetic energy at burn is supported by measurements of neutron peak shifts, which demonstrate the absence of directional velocity for this type of implosion.²⁴ As an example, the MRS-measured spectrum from shot 85 481 is shown in Fig. 3, together with a forward fit to the data using a Gaussian model for the neutron spectrum folded with the Geant4-simulated response function (solid red curve). $T_{\text{ion}} = 11.4 \pm 0.3(\text{stat})$ keV is inferred from the fit.

Also plotted in Fig. 3 is the full simulated MRS response to a mono-energetic 14 MeV neutron (dashed red line). As expected, given the simulated MRS resolution in this configuration of 0.91 MeV, the response represents a substantial fraction of the width of the measured peak. The majority of this broadening is due to the ion optical properties of the magnet. If only kinematic and foil broadening are considered, the blue broken curve in Fig. 3 is obtained (FWHM = 0.44 MeV).

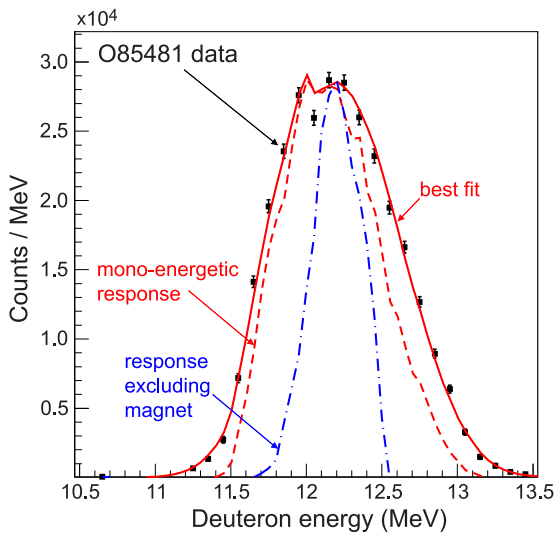


FIG. 3. MRS-measured spectrum from OMEGA shot 85 481 (black points). A forward fit to the data (solid red curve) gives $T_{\text{ion}} = 11.4 \pm 0.3(\text{stat})$ keV. Also shown are the Geant4-simulated response for a mono-energetic 14 MeV neutron (dashed red curve) and the response considering only the foil and aperture geometry (excluding the magnet) as simulated using MCNP (blue broken curve).

It is worth noting that without the systematic foil misalignment in the non-dispersion direction, a slightly better $\Delta E_{\text{MRS}} = 0.88$ MeV is calculated, and without the detector misplacement relative to the magnet focal plane, $\Delta E_{\text{MRS}} = 0.72$ MeV.

MRS and nTOF-inferred T_{ion} from the full implosion series are contrasted in Fig. 4. Here, the nTOF numbers represent the average of measurements using 6 nTOF detectors in different LOSs,²⁵ with the standard deviation taken as the uncertainty. The thin black MRS error bars represent the statistical uncertainty in the MRS analysis and the gray error bars represent the systematic uncertainty. The systematic uncertainty can be derived²⁶ to be

$$\sigma_{T_{\text{ion}}} = 2 \times \left(\frac{\sigma_{\Delta E_{\text{MRS}}}}{\Delta E_{\text{MRS}}} \right) \frac{1}{177^2} \Delta E_{\text{MRS}}^2, \quad (1)$$

where $\sigma_{\Delta E_{\text{MRS}}}/\Delta E_{\text{MRS}}$ is the uncertainty in the resolution. Table I summarizes the systematic uncertainty for the 4 cm², 57.2 μm OMEGA MRS foil configuration, which can be divided into three separate categories: (i) “fixed uncertainty” (top section in Table I), which represents factors that are not expected to change significantly over time, (ii) CR-39 alignment uncertainty, which changes from shot to shot, and (iii) uncertainty due to foil alignment variations. The CR-39 alignment uncertainty arises because the primary peak splits across two pieces of CR-39 (W9 and W10) that are independently processed with an estimated combined alignment uncertainty (from fielding and scanning) of ± 50 μm relative to each other. (In Fig. 3, the stitch between the two pieces is at ~ 12 MeV.)

The simulated impact of foil alignment variations on the primary deuteron peak location and MRS resolution is summarized in Fig. 5, where it is plotted separately for foil changes in the dispersion direction (nominal location $x = 0$ cm) and the non-dispersion direction (nominal location $y = -0.6$ cm). A second set of experiments using the 4 cm², 57.2 μm foil was tried seven months after the results reported here were obtained, and the primary deuteron peak was found to have shifted systematically by 0.22 MeV, while the signal

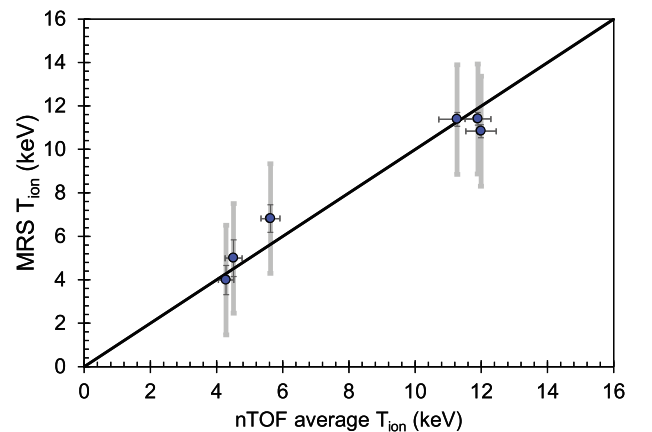


FIG. 4. MRS vs nTOF-measured T_{ion} . The nTOF numbers represent the average of measurements using 6 nTOF detectors in different lines-of-sight, with the standard deviation taken as the uncertainty. The narrow black MRS error bar is the statistical uncertainty and the broader gray error bar is the estimated systematic uncertainty.

TABLE I. Parameters impacting the MRS spectral resolution ΔE_{MRS} and its uncertainty $\sigma_{\Delta E_{\text{MRS}}}$ and the resulting inferred systematic uncertainty in the T_{ion} measurement ($\sigma_{T_{\text{ion}}}$).

MRS parameter	Nominal value	Parameter uncertainty	$\sigma_{\Delta E_{\text{MRS}}}/\Delta E_{\text{MRS}}$ (%)
Foil dist. (cm)	10	± 0.3	± 3.34
Foil radius (cm)	1.13	± 0.025	± 1.88
Foil thickness (μm)	57.2	± 2.0	± 1.74
Foil density (g/cm^3)	1.08	± 0.01	± 0.73
Aperture area (cm^2)	21.3	± 0.2	± 0.65
Magnet dist. (cm)	225	± 0.2	± 0.39
Total			± 4.34
$\sigma_{T_{\text{ion}}}$ (keV)		± 2.3	
CR-39 alignment (μm)	0	± 50	± 1.93
$\sigma_{T_{\text{ion}}}$ (keV)		± 1.0	
Foil alignment (cm)	0	± 0.5	± 9.74
$\sigma_{T_{\text{ion}}}$ (keV)		± 5.2	

distributions remained identical in the non-dispersion direction. This indicates an unintended foil shift of 0.5 mm in the dispersion direction between these two shot days [Fig. 5(a)]. As can be seen from Table I, such uncontrolled foil shifts introduce substantial uncertainty in the T_{ion} measurement.

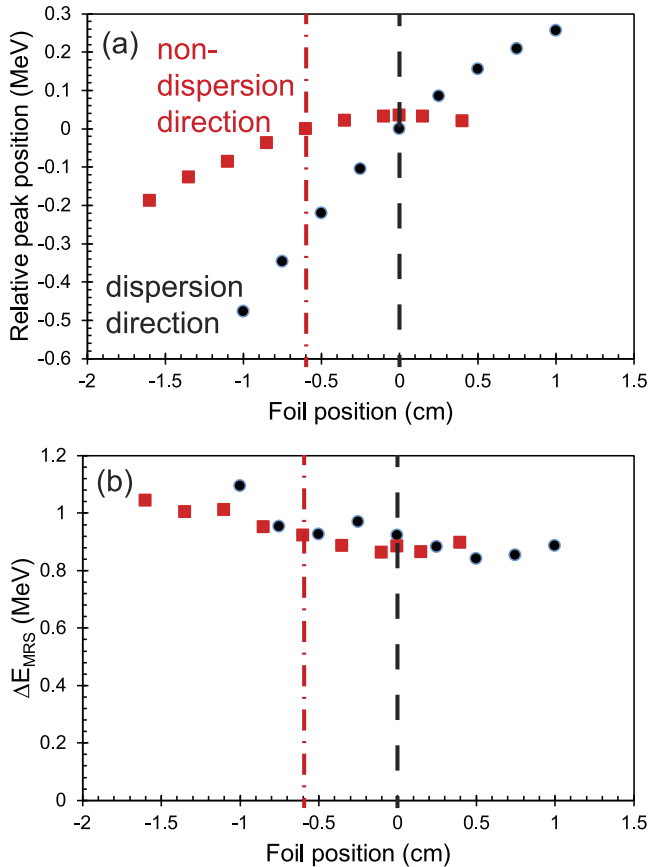


FIG. 5. (a) Relative position of the primary deuteron peak and (b) FWHM resolution ΔE_n as a function of foil position for foil shifts in the dispersion (black) and non-dispersion (red) directions. The nominal foil position (indicated with vertical lines) is taken to be 0 cm in the dispersion direction (dashed line) and -0.6 cm in the non-dispersion direction (broken line).

The systematic uncertainty plotted in Fig. 4 includes only fixed parameter uncertainty and the CR-39 alignment uncertainty, which varies randomly from shot to shot. It does not include foil alignment uncertainty, because the foil alignment was specifically verified immediately prior to this experiment. The observed uncontrolled foil alignment shift indicates that such alignment verifications need to be routinely performed.

IV. PROPOSED SYSTEM IMPROVEMENTS

The agreement between MRS and nTOF-inferred T_{ion} for the preliminary MRS measurements presented here is found to be excellent within the quoted error bars (Fig. 4, $\chi^2_{\text{red}} = 0.1$ if the full error bars are considered). This reassuring result indicates good understanding of the very different systematics associated with the two independent measurements. However, to truly contribute to constraining the T_{ion} measurements, the MRS error bars need to be substantially reduced. From Eq. (1), it is clear that this could be achieved by improving the MRS resolution. Reducing the associated uncertainties is also important.

As discussed above, the MRS resolution can be separated into three components, ΔE_{kin} , ΔE_{foil} , and ΔE_{mag} . ΔE_{kin} and ΔE_{foil} could be reduced by reducing the foil opening angle and using a thinner foil, respectively. However, either of these choices would also lead to reduced efficiency, as the MRS efficiency is directly proportional to the foil solid angle and thickness. It has also been demonstrated above that the dominant broadening source for the 4 cm^2 foil setup is ΔE_{mag} (Fig. 3). The focusing properties of the MRS magnet are, in principle, more favorable for a smaller particle source. Thus, an interesting approach to improving MRS resolution at maintained efficiency is to field a smaller foil closer TCC, with a maintained solid angle. VisRad²⁷ has been used to verify that a $\phi = 1 \text{ mm}$ foil could be placed 0.5 cm from TCC in the MRS LOS without clipping any laser beams when the standard SG5 phase plates are used (in fact, the tightest tolerance is to beam B29, which could handle a foil up to 0.6 mm radius). The foil could be placed in the MRS line-of-sight using a ten-inch-manipulator (TIM) target inserter and a standard $17 \mu\text{m}$ SiC stalk. A similar foil 5 mm from TCC has been extensively used for backlighting experiments,²⁸ demonstrating the feasibility of this approach. However, testing would be required before implementation with MRS to ensure the foil survives long enough to produce recoil deuterons. Geant4-simulated recoil deuteron distributions (with $T_{\text{ion}} = 2 \text{ keV}$) for this foil geometry are illustrated in Fig. 6. The inferred resolution with the as-built MRS geometry is $\Delta E_{\text{MRS}} = 0.80 \text{ MeV}$, which is not significantly better than that for the 4 cm^2 foil case; this is because the detectors are not located in the focal plane of the magnet. For the nominal MRS geometry, $\Delta E_{\text{MRS}} = 0.45 \text{ MeV}$ in this configuration, with combined broadening due to the foil and kinematics at 0.37 MeV , meaning the magnet is no longer the dominant broadening source. Broadening could be further reduced by using a thinner foil, although at a direct cost in efficiency.

It is clear that to be able to exploit the gain in resolution obtained by a smaller, closer foil with the existing MRS,

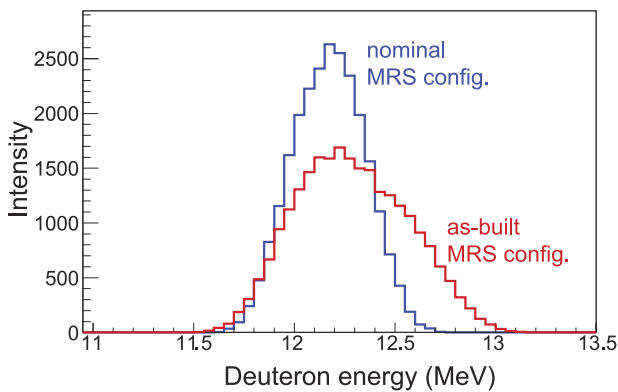


FIG. 6. Simulated recoil deuteron spectra using the nominal MRS geometry (blue) and the as-built MRS geometry (red) with a $57.2\ \mu\text{m}$ thick foil.

the detector array would have to be redesigned. The distance between nominal and as-built foil locations for W9 and W10 is only ~ 3 cm, meaning there is most likely enough room to redesign the detector array within the existing hardware envelope. A detector redesign should also include optimization to capture the primary peak on a single CR-39 coupon, which would eliminate the CR-39 alignment uncertainty (see Table I).

The closer foil geometry would also place the foil within the field of view of the OMEGA precision target viewing system, which could be exploited to reduce uncertainty in the foil location and distance from TCC—these two factors are seen in Table I to contribute substantially to $\sigma_{\Delta E_{\text{MRS}}}/\Delta E_{\text{MRS}}$.

V. SUMMARY AND CONCLUSIONS

In this paper, we have shown that T_{ion} measurements using the OMEGA MRS fielded with a new, $4\ \text{cm}^2$, $57.2\ \mu\text{m}$ -thick conversion foil are in excellent agreement with nTOF T_{ion} measurements within the associated uncertainties, indicating good understanding of the systematics associated with the two independent measurements. However, the MRS resolution in this configuration $\Delta E_{\text{MRS}} = 0.91\ \text{MeV}$ is too poor for a high-precision measurement. With a redesigned detector array and a smaller foil at 5 mm from TCC, the MRS resolution could be reduced to $\Delta E_{\text{MRS}} = 0.45\ \text{MeV}$ at maintained efficiency. This would automatically reduce the systematic T_{ion} uncertainty, $\sigma_{T_{\text{ion}}}$, by a factor 4 [Eq. (1)]. Further reduction in $\sigma_{T_{\text{ion}}}$ is also obtained in this configuration by reducing foil positioning uncertainty and eliminating CR-39 alignment uncertainty.

ACKNOWLEDGMENTS

The authors would like to thank the OMEGA operations crew for executing the experiments reported herein and Ernie Doeg, Robert Frankel, and Michelle McCluskey for

processing of the CR-39 data used in this work. This material is based upon work supported by the Department of Energy, National Nuclear Security Administration under Award No. DE-NA0002949 and by LLE under Award No. 415935-G, and work performed under the auspices of the U.S. Department of Energy by General Atomics under Contract No. DE-NA0001808. This report was prepared as an account of work sponsored by an agency of the United States Government. Neither the United States Government nor any agency thereof, nor any of their employees, makes any warranty, express or implied, or assumes any legal liability or responsibility for the accuracy, completeness, or usefulness of any information, apparatus, product, or process disclosed, or represents that its use would not infringe privately owned rights. Reference herein to any specific commercial product, process, or service by trade name, trademark, manufacturer, or otherwise does not necessarily constitute or imply its endorsement, recommendation, or favoring by the United States Government or any agency thereof. The views and opinions of authors expressed herein do not necessarily state or reflect those of the United States Government or any agency thereof.

- ¹T. R. Boehly *et al.*, *Opt. Commun.* **133**, 495 (1997).
- ²J. A. Frenje *et al.*, *Rev. Sci. Instrum.* **73**, 854 (2001).
- ³J. A. Frenje *et al.*, *Rev. Sci. Instrum.* **79**, 10E502 (2008).
- ⁴J. A. Frenje *et al.*, *Phys. Plasmas* **17**, 056311 (2010).
- ⁵D. T. Casey *et al.*, *Rev. Sci. Instrum.* **83**, 10D912 (2012).
- ⁶D. T. Casey *et al.*, *Rev. Sci. Instrum.* **84**, 043506 (2013).
- ⁷C. Forrest *et al.*, *Rev. Sci. Instrum.* **83**, 10D919 (2012).
- ⁸V. Yu. Glebov, C. J. Forrest, K. L. Marshall, M. Romanofsky, T. C. Sangster, M. J. Shoup III, and C. Stoeckl, *Rev. Sci. Instrum.* **85**, 11E102 (2014).
- ⁹C. J. Forrest *et al.*, *Rev. Sci. Instrum.* **87**, 11D814 (2016).
- ¹⁰R. Betti *et al.*, *Bull. Am. Phys. Soc.* **62**, 12 (2017), <http://meetings.aps.org/link/BAPS.2017.DPP.TI.2.1>.
- ¹¹S. P. Regan *et al.*, *Phys. Rev. Lett.* **117**, 025001 (2016).
- ¹²L. Ballabio, J. Källne, and G. Gorini, *Nucl. Fusion* **38**, 1723 (1998).
- ¹³T. J. Murphy, *Phys. Plasmas* **21**, 072701 (2014).
- ¹⁴B. Appelbe and J. Chittenden, *Plasma Phys. Controlled Fusion* **53**, 045002 (2011).
- ¹⁵M. Gatu Johnson *et al.*, *Phys. Rev. E* **94**, 021202(R) (2016).
- ¹⁶I. V. Igumenshchev *et al.*, *Phys. Plasmas* **23**, 052702 (2016).
- ¹⁷I. V. Igumenshchev, *Phys. Plasmas* **24**, 056307 (2017).
- ¹⁸R. C. Shah *et al.*, *Phys. Rev. Lett.* **118**, 135001 (2017).
- ¹⁹V. N. Goncharov *et al.*, *Plasma Phys. Controlled Fusion* **59**, 014008 (2017).
- ²⁰B. M. Van Wontergem *et al.*, *Fusion Sci. Technol.* **69**, 452–469 (2016).
- ²¹M. Gatu Johnson *et al.*, *Rev. Sci. Instrum.* **83**, 10D308 (2012).
- ²²M. Gatu Johnson *et al.*, *Rev. Sci. Instrum.* **87**, 11D816 (2016).
- ²³S. Agostinelli *et al.*, *Nucl. Instrum. Methods Phys. Res. A* **506**(3), 250 (2003).
- ²⁴O. Mannion, V. Yu. Glebov, C. J. Forrest, J. P. Knauer, V. N. Goncharov, S. P. Regan, T. C. Sangster, C. Stoeckl, and M. Gatu Johnson, “Calibration of a neutron time-of-flight detector with a rapid instrument response function for measurements of bulk fluid motion on OMEGA,” *Rev. Sci. Instrum.* (these proceedings).
- ²⁵V. Yu. Glebov, “Six DT nTOF detectors on OMEGA,” nTOF Diagnostic Workshop, LLNL, July 18, 2017.
- ²⁶O. N. Jarvis, *Diagnostics for Fusion Reactor Conditions* (Pergamon Press, Varenna, 1982), EUR 8351 EN 1982.
- ²⁷J. J. MacFarlane, *J. Quant. Spectrosc. Radiat. Transfer* **81**, 287 (2003).
- ²⁸C. Stoeckl *et al.*, *Rev. Sci. Instrum.* **85**, 11E501 (2014).